



This is a repository copy of *A Mechanistic Study of the Lewis Base-Directed Cycloaddition of 2-Pyrones and Alkynylboranes*.

White Rose Research Online URL for this paper:
<http://eprints.whiterose.ac.uk/90396/>

Version: Accepted Version

Article:

Crepin, D.F.P., Harrity, J.P.A., Jiang, J. et al. (3 more authors) (2014) A Mechanistic Study of the Lewis Base-Directed Cycloaddition of 2-Pyrones and Alkynylboranes. *Journal of the American Chemical Society*, 136 (24). 8642 - 8653. ISSN 0002-7863

<https://doi.org/10.1021/ja501805r>

Reuse

Unless indicated otherwise, fulltext items are protected by copyright with all rights reserved. The copyright exception in section 29 of the Copyright, Designs and Patents Act 1988 allows the making of a single copy solely for the purpose of non-commercial research or private study within the limits of fair dealing. The publisher or other rights-holder may allow further reproduction and re-use of this version - refer to the White Rose Research Online record for this item. Where records identify the publisher as the copyright holder, users can verify any specific terms of use on the publisher's website.

Takedown

If you consider content in White Rose Research Online to be in breach of UK law, please notify us by emailing eprints@whiterose.ac.uk including the URL of the record and the reason for the withdrawal request.



eprints@whiterose.ac.uk
<https://eprints.whiterose.ac.uk/>

A Mechanistic Study of the Lewis Base Directed Cycloaddition of 2-Pyrones and Alkynylboranes

Damien F. P. Crépin,[†] Joseph P. A. Harrity,^{*,†} Julong Jiang,[†] Anthony J. H. M. Meijer,^{*,†} Anne-Chloé M. A. Nassoy[†] and Piotr Raubo[‡]

[†]Department of Chemistry, University of Sheffield, Sheffield, S3 7HF, U. K.

[‡]Research and Development, AstraZeneca, Alderley Park, Macclesfield, SK10 4TG, U.K.

a.meijer@sheffield.ac.uk

j.harrity@sheffield.ac.uk

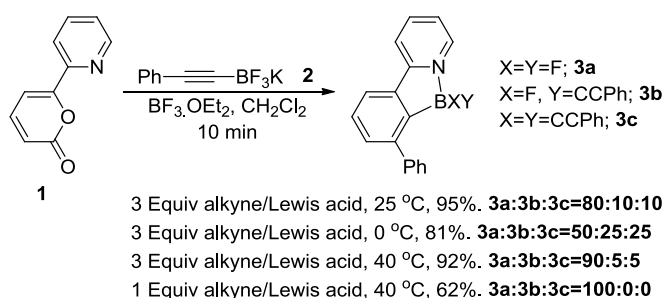
Abstract: Significant rate enhancements in the Diels-Alder reaction of alkynes and 2-pyrones bearing a Lewis basic group are observed when a combination of alkynyltrifluoroborates and $\text{BF}_3 \cdot \text{OEt}_2$ are used. This process generates functionalized aromatic compounds with complete regiocontrol. The origin of the observed rate enhancement has been studied by DFT methods, and they appear to originate for coordination of the diene substrate to a mixture of alkynylborane intermediates, followed by a Lewis acid mediated product equilibration step. Evidence for this mechanism is presented, as is the enhanced promotion of the cycloaddition via the use of alternative Lewis acid promoters.

Introduction

The Diels-Alder cycloaddition of 2-pyrones represents an efficient method of generating functionalised cyclohexenes,¹ and was first described by Diels and Alder over 80 years ago.² This reaction also offers an effective method for the synthesis of highly substituted aromatic compounds when alkynes are employed, whereby the intermediate cycloadduct undergoes rapid retro-cycloaddition and expulsion of carbon dioxide.³ A range of alkynes are known to participate in this process including those bearing hydrocarbon, ester, ketone,³ boronate,⁴ stannane⁵ and silyl⁶ groups. A significant challenge in this chemistry is the requirement of high reaction temperatures over extended time periods, and variable reaction regiocontrol. Such limitations are addressed only by the use of very reactive dienophiles such asynamides,⁷ thereby restricting the scope of products that can be generated by this strategy.

Recent studies in our labs have sought to address the high temperatures required in [4 + 2] cycloaddition reactions of aromatic dienes by virtue of a Lewis acid-base complex induced promotion of this process.⁸ This approach has the added advantage of generating compounds with complete regiocontrol. We have developed a mild and regioselective synthesis of aromatic difluoroboranes via the cycloaddition of 2-pyrones with in situ generated alkynyldifluoroboranes.⁹ As outlined in Scheme 1, our optimization studies highlighted some unexpected trends; the reaction required the use of 3 equivalents of both the alkyne substrate and the Lewis acid fluorophile for optimal yields. Moreover, alkynylated by-products were observed when the reaction was conducted under ambient conditions. In this context, the mild Diels-Alder cycloaddition of 1,3-dienes with vinyl- and alkynylboranes has also been established by Singleton and co-workers. These processes take place at ambient temperature and with excellent levels of regiocontrol via a [4 + 3] transition structure.¹⁰

Scheme 1 The Lewis acid promoted cycloaddition of 2-pyrones.



The directed cycloaddition reaction raised some interesting questions with regard to the reaction mechanism: 1) Is Lewis acid activation of the 2-pyrone operating as well as, or instead of, the directed cycloaddition? 2) Does the directing group control reaction regioselectivity or does the reaction proceed via Singleton [4 + 3] mechanism? 3) How are the alkynylated by-products formed? In order to understand this reaction more clearly, we undertook theoretical DFT calculations of the cycloaddition reaction in order to establish a clearer picture of this unusually rapid cycloaddition process. Theoretical studies of Lewis-acid promoted Diels-Alder reactions have been reported in the literature,¹¹ though not on these systems. We report herein our findings and their application in improving the Lewis acid promoted cycloaddition reaction.

Computational methods

All calculations were performed at the DFT level of theory, by means of the hybrid B3LYP¹²⁻¹³ functional as implemented in *Gaussian09*¹⁴. The 6-311G(d,p) basis set was used for the atoms H, C, N, O, B, F and Cl. All structures of reactants, intermediates, transition states and products were fully optimized without any symmetry restrictions. Transition states were located using the QST3 algorithm¹⁵⁻¹⁷ or the Berny algorithm¹⁸.

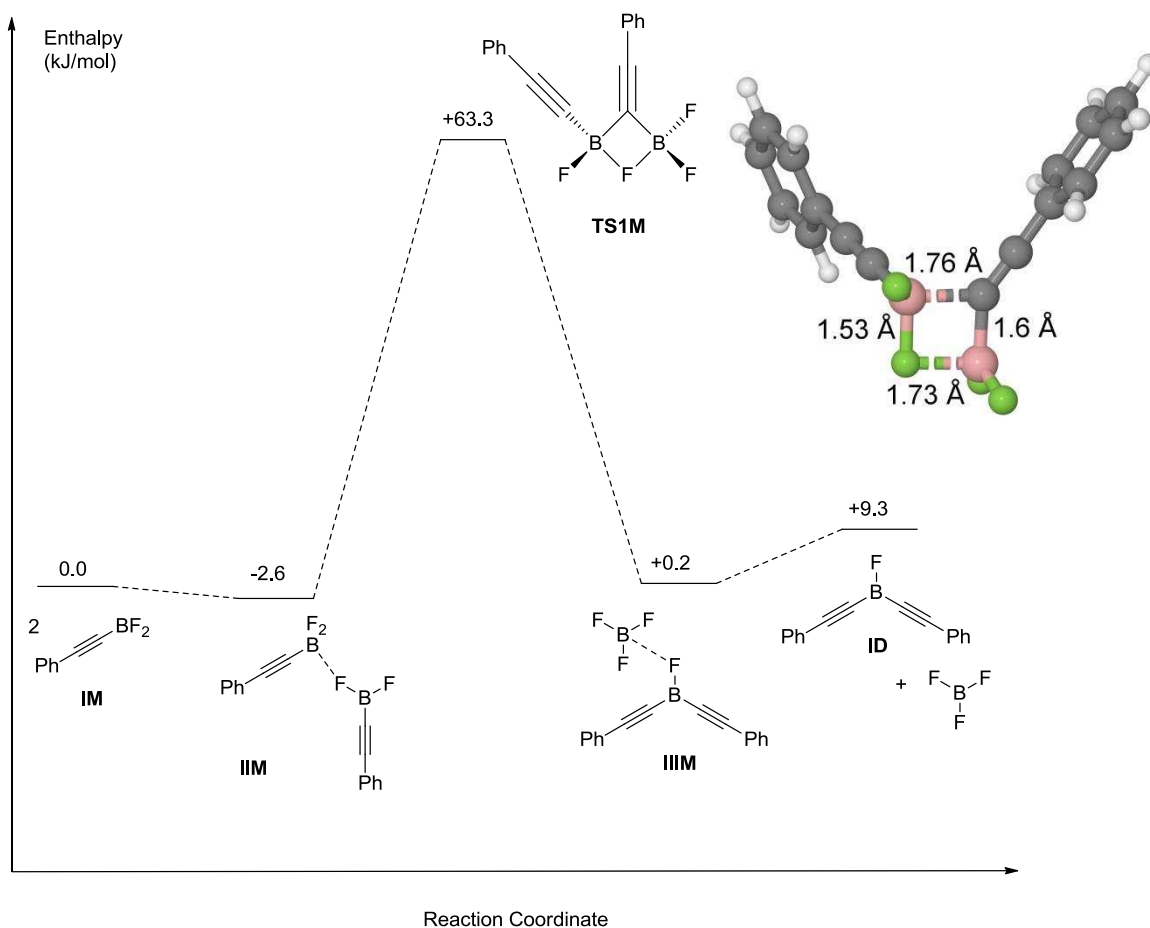
A frequency calculation was carried out to characterize all optimized structures as local minima or transition states. Transition states were identified by having one imaginary frequency. An intrinsic reaction coordinate (IRC)¹⁹ calculation was performed for each of the transition states to ensure that a given transition state connected the correct reactants and products. Solvent effects were included in all calculations through the IEF-PCM²⁰⁻²² model implemented in *Gaussian09*¹⁴ with dichloromethane (DCM) as solvent. The atomic charges were fitted to the electrostatic potential energy (ESP) following the Merz-Kollman scheme.^{23,24} All enthalpies and free energies quoted below were evaluated at 298.15 K

Theoretical Results

Our first objective was to attempt to explore possible mechanisms for the formation of the alkynylated aromatic boranes such as **3b,c** shown in Scheme 1. Our initial hypothesis involved alkyne disproportionation prior to cycloaddition. However, Frohn and co-workers had shown that alkynyl difluoroboranes can be isolated and characterised as single compounds upon the treatment of alkynyl trifluoroborates with boron trifluoride.²⁵ Nevertheless, alkyne exchange between organoboranes and –borates has been reported by Negishi *et al.*²⁶ First, the ligand exchange reaction between two alkynylborane **IM** monomers

was considered. Following Ref. 27a, the enthalpy profile for the ligand exchange reaction between two alkynylborane **IM** monomers is shown in Scheme 2.

Scheme 2 The energy profile of the ligand exchange between two alkynylborane (monomer **IM**) molecules in DCM. The inset shows the transition state **TS1M** structure, where the bonds forming are dashed.

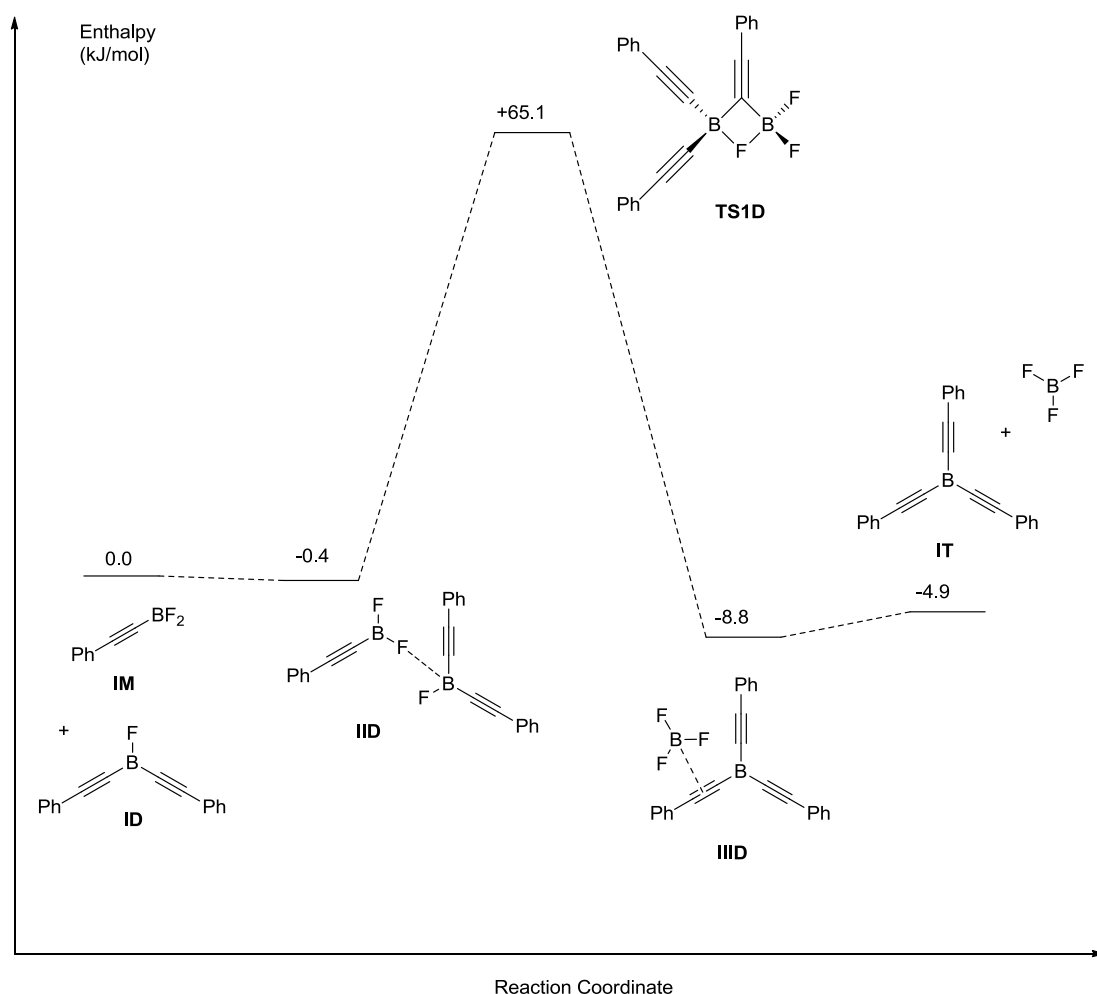


In non-polar solvents like dichloromethane, the alkynylboranes will form a loosely coordinated dimer **IIM**, which results in a small enthalpy change of -2.6 kJ mol^{-1} . This pre-reaction complex then undergoes ligand exchange to generate bis(alkynyl)borane **ID** and a molecule of BF_3 . Inspection of the transition state (**TS1M**) of this process shows that this reaction involves a concerted mechanism via a four-membered ring involving two three-centre two-electron bonds (Scheme 2). The enthalpic barrier for the ligand (phenylacetylide moiety) exchange between two alkynylborane molecules is calculated to be $+65.9 \text{ kJ mol}^{-1}$ from the loosely coordinated dimer **IIM**. The product of this process **IIIIM** is again a loosely bound complex. However, this complex is a dimer of the diphenylacetylide **ID** and BF_3 , whereby BF_3 prefers to bind with the fluoride of **ID**. The calculations clearly show that the

formation of bis(alkynyl)borane from two alkynylborane molecules is an endoergic process, since the Gibbs energy increases overall by 13.2 kJ mol⁻¹ compared to two individual alkynylborane molecules. Therefore, for this process to be viable it must be coupled with the Diels-Alder cycloaddition step (*vide infra*).

Following a similar pathway, the tris(alkynyl)borane **IT** can be formed from either an alkynylborane **IM**/bis(alkynyl)borane **ID** disproportionation, or by ligand exchange from two bis(alkynyl)borane **ID** molecules. The likely relative concentrations of **IM** and **ID** suggest that ligand exchange is more likely to happen via the reaction of **IM** and **ID**. Thus, the intermediates and transition states along this reaction pathway were optimized. The energy profile for the generation of tris(alkynyl)borane is shown in Scheme 3.

Scheme 3 The energy profile of the ligand exchange between an alkynylborane molecule (**IM**) and a bis(alkynyl)borane molecule (**ID**) in DCM.



The enthalpy barrier for this disproportionation reaction is $+65.5 \text{ kJ mol}^{-1}$. It again delivers a loosely coordinated product. Dissociation of this complex provides free tris(alkynyl)borane **IT**, which is available to participate in the subsequent Diels-Alder reaction. We note that in this case the overall reaction Gibbs energy is negative (-2.5 kJ mol^{-1}). Thus, our calculations show that equilibration of a series of alkynylboranes can take place, and that this equilibrium favours the formation of trisalkynylborane **IT** and its corresponding BF_3 -complex **IIID**. This needs to be taken into account when studying the subsequent Diels-Alder reaction.

Having established the potential for rapid alkyne equilibration via disproportionation, we envisaged that the cycloadduct product distribution would depend on the relative energies of the pyrone-complexed trivalent boranes, as well as the activation energy of the ensuing cycloaddition. Therefore, we turned our attention to the Diels-Alder step adopting either alkynylborane, bis(alkynyl)borane and tris(alkynyl)borane as the dienophile and the 2-pyrone 3-N,N-dimethyl-2-oxo-2H-pyran-6-carboxamide (**S1**) as the diene.

The mapped energy profile for the Diels-Alder reaction between alkynylborane **IM** with **S1** is shown in Scheme 4. The first step in this regio-directing Diels-Alder reaction is the coordination of the amide carbonyl directing group of the 2-pyrone to the boron atom of the alkynylborane. This step lowers the enthalpy by $-37.9 \text{ kJ mol}^{-1}$. The subsequent Diels-Alder reaction therefore proceeds via this pre-reaction complex **IM_DA_I1**. Inspection of the cycloaddition transition state (**IM_DA_TS1**) shows that the Diels-Alder reaction can be described as asynchronous. Thus, the two bonds C_1-C_A , C_2-C_B do not form simultaneously. In the optimized TS structure, the bond length of C_1-C_A is 1.81 \AA while the distance between C_2 and C_B is still as large as 2.97 \AA as is clear from Figure 1(a). Thus, our calculations clearly indicate that the reaction *via* a directed $[4 + 2]$ mechanism rather than the Singleton $[4 + 3]$ mechanism.

Scheme 4 The energy profile of the regio-directing Diels-Alder reaction between alkynylborane (**IM**) and 2-pyrone (**S1**) in DCM. Inset shows structure of **IM_DA_I2**.

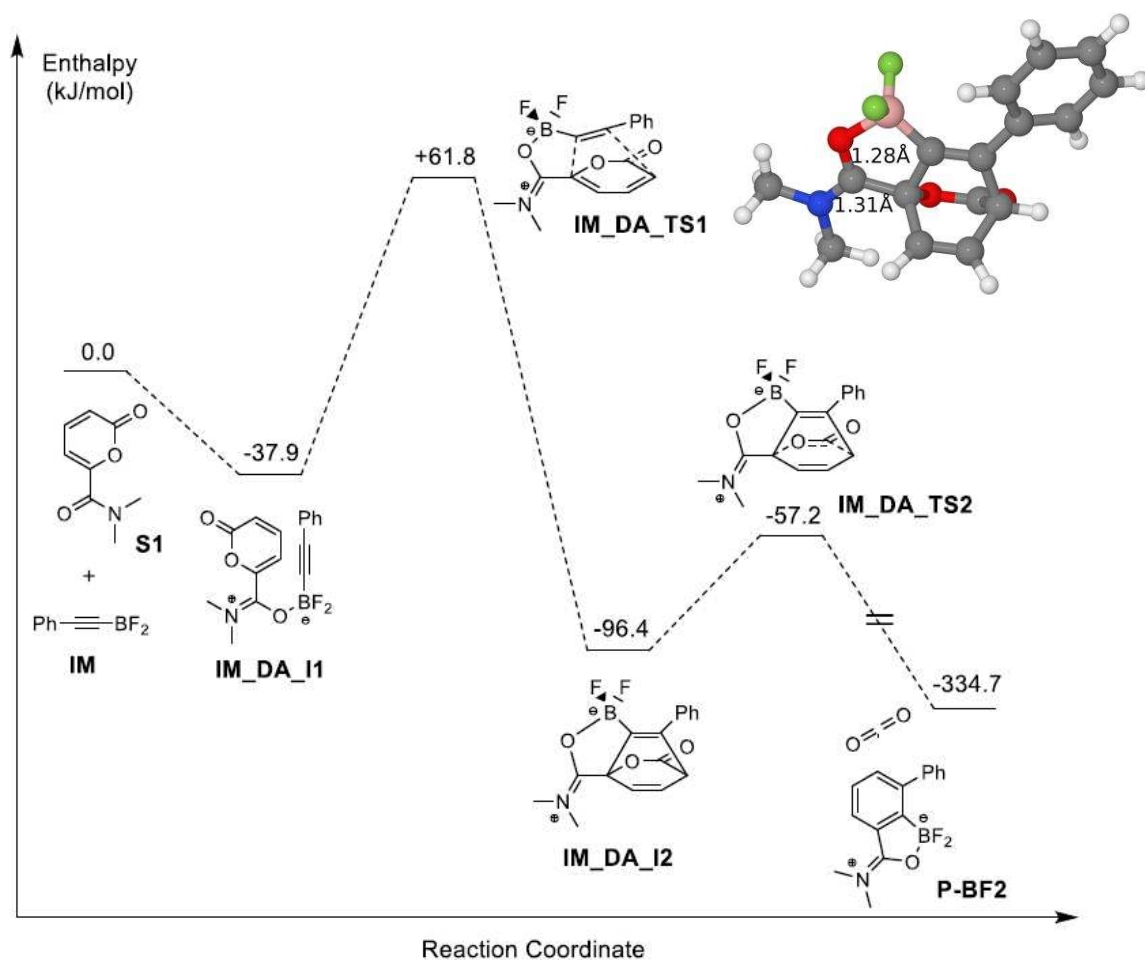
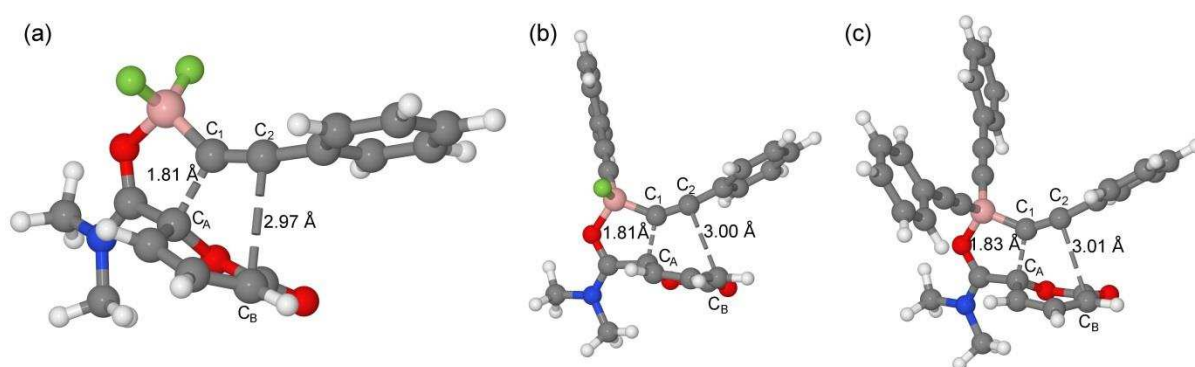


Figure 1 The three transition states of the Diels-Alder reaction. Panel (a): reaction of **IM** with **S1**. Panel (b): reaction of **ID** with **S1**. Panel (c): reaction of **IT** with **S1**.



ESP charges based on the Merz-Kollman scheme (*vide infra*; Table 2) clearly indicate the C₁-C_A bond is formed by a nucleophilic attack from the C₁ atom on the phenylacetylide group to the C_A atom on the 2-pyrone ring, leading to a polar intermediate. Such stepwise [4 + 2]

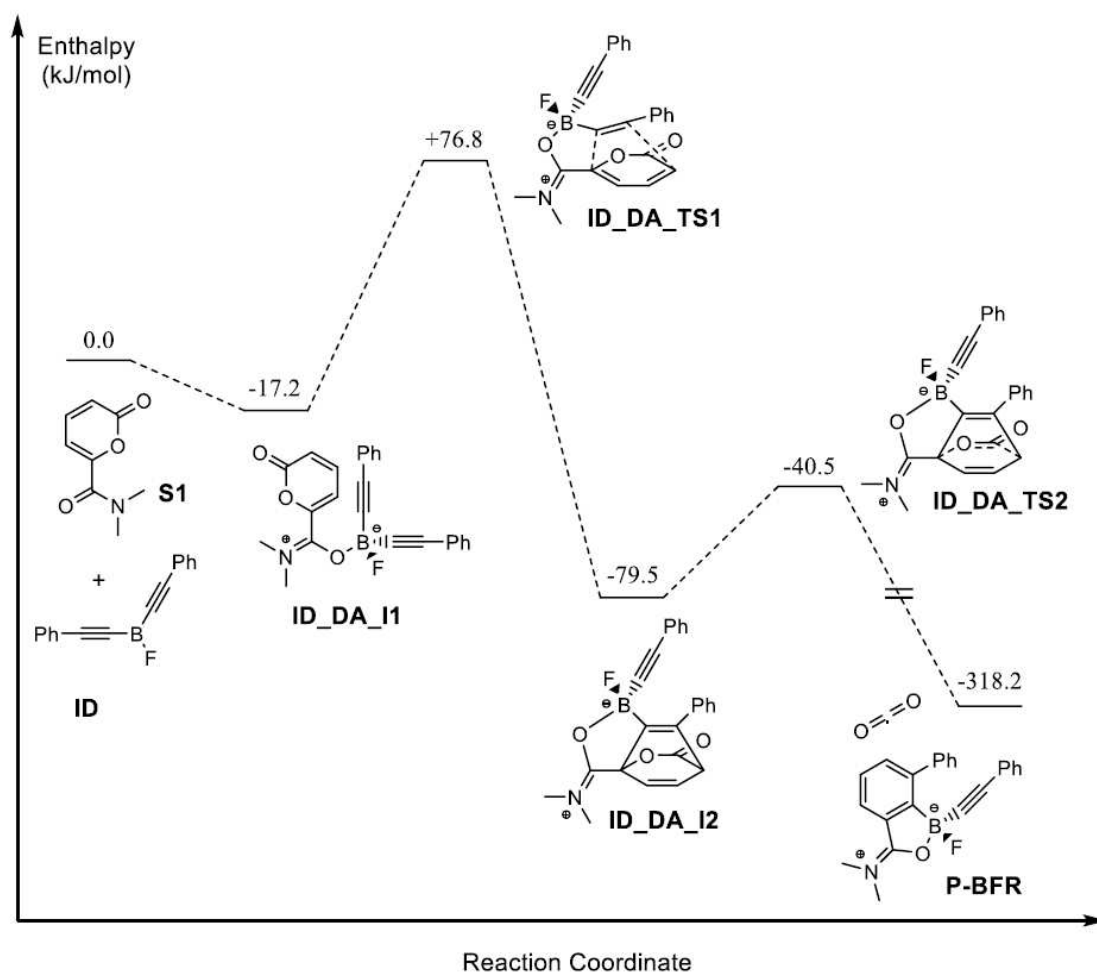
cycloadditions of 2-pyrones are known and have been studied by DFT methods in the past.²⁷ Finally, the product of this cyclisation reaction is a bridged compound **IM_DA_I2** which is shown in the inset of Scheme 4. It is worth noting that the O-C bond length of the carbonyl group in this bridged compound extends to 1.28 Å and that the N-C bond on the other hand shortens to 1.31 Å, which is quite similar to a C=N double bond. However, this bridged compound **IM_DA_I2** is not stable towards release of CO₂. The barrier for the CO₂ release and rearrangement of the aromatic ring is +39.2 kJ mol⁻¹ while the enthalpy change for this step is -238.2 kJ mol⁻¹.

We have also studied the related pathways of this regioselective Diels-Alder reaction starting with the bis(alkynyl)borane **ID** or the tris(alkynyl)borane **IT**. The corresponding enthalpy profiles are shown in Scheme 5 and Scheme 6, respectively. Comparing Scheme 5 and 6 to each other and to Scheme 4 shows some similarities and some differences between the three reactions. For Scheme 5, like for Scheme 4, the initial step is the formation of a pre-reaction complex, whereby it needs to be noted that the enthalpy change for Scheme 4 is about twice as large as for Scheme 5. It is therefore not surprising that the formation of this pre-reaction complex is actually endothermic for **IT**, as is evident from Scheme 6. The transition states for each of the three schemes on the other hand shows that the Diels-Alder reaction can be described as asynchronous in each case forming one C-C bond before the second one. In all three cases the bridged product of the DA reaction is not stable and should lose CO₂ quite easily, given the relative barrier of ~40 kJ mol⁻¹ in each case with a large reaction enthalpy.

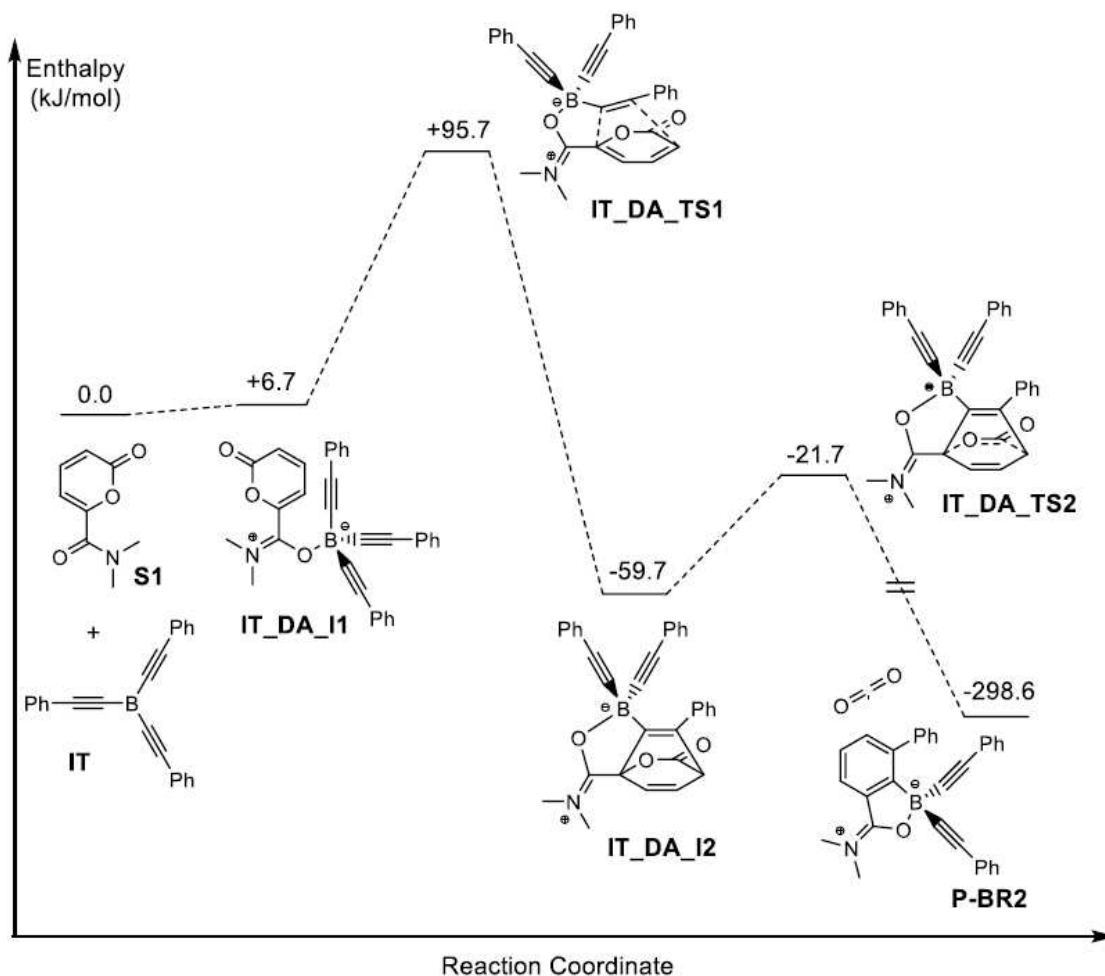
To be able to compare these reactions quantitatively, it is necessary to be able to define an effective barrier in each case. This can be less than straightforward, particularly when there are multiple transition states and minima to consider. Thus, in order to assign a barrier consistently, we use the Energetic Span (ES) model developed by Kozuch.²⁸⁻³⁰ Within the ES model, the crucial states (i.e. stationary points on the potential energy surface) of the system are those that give the maximum energy difference between a minimum and a subsequent transition state, i.e. give you the maximum effective barrier or energetic span for the reaction.²⁸⁻³⁰ Thus, for Scheme 4, those states are **IM_DA_I1** and **IM_DA_TS1**, which are referred to as the turnover determining intermediate (TDI) and turnover determining transition state (TDTS), respectively. As a result, the effective barrier for this reaction is 99.7 kJ mol⁻¹.

Scheme 5 The energy profile of the regio-directing Diels-Alder reaction between

bis(alkynyl)borane (**ID**) and 2-pyrone (**S1**).



Scheme 6 The energy profile of the regio-directing Diels-Alder reaction between tri(alkynyl)borane (**IT**) and 2-pyrone (**S1**).



For Scheme 5 and Scheme 6, it is clear that the transition state (TS) of the cyclisation step, i.e. ID_DA_TS1 and IT_DA_TS1, respectively, is the TDTS. For Scheme 5, the pre-reaction complex is the TDI, whereas for Scheme 6, the separated reactants form the TDI. Therefore, the effective barrier, i.e. the energetic difference between TDTS and TDI, for Scheme 5 and Scheme 6 are calculated to be +94.0 and +95.7 kJ mol⁻¹, respectively.

Combining the results of our theoretical studies on both the ligand-exchange pathway and the Diels-Alder reaction, it is now clear why a mixture of aromatic boranes is formed. Compared to the cycloaddition step, the ligand exchange process allows for rapid equilibration of the various alkynylborane intermediates. The relative rates of cycloaddition of these alkynylboranes then determines the distribution of initial cycloadducts. As shown by the data in Table 1, the effective barrier decreases with ligand exchange of fluoride for acetylide, which means that the rate will increase accordingly. Assuming that the reaction proceeds under kinetic control, relative reaction rates can be calculated using the Eyring equation.

These results are shown in the third column of Table 1. If we assume that changes in entropy are similar for all three reactions, then we can define a relative rate based on the enthalpy alone. These relative rates are given in the fifth column of Table 1. It is clear from Table 1 that either calculation gives qualitatively the same results, namely that the reaction rates for **ID** and **IT** are similar and much larger than the rate for **IM**.

Table 1 The effective barriers (energetic spans) for the Diels-Alder reaction with different dienophiles

Dienophile	ΔG^\ddagger ($\frac{\text{kJ}}{\text{mol}}$)	Relative rate	ΔH^\ddagger ($\frac{\text{kJ}}{\text{mol}}$)	Relative rate
Alkynylborane (IM)	109.5	1.0	99.7	1.0
Bis(alkynyl)borane (ID)	100.7	34.8	94.0	10.0
Tris(alkynyl)borane (IT)	100.4	39.3	95.7	5.0

Inspection of the energy profiles in Schemes 4-6 shows a clear dependency of the enthalpy of activation on the nature of the ligands around boron. In order to rationalize this result, an ESP (Merz-Kollman) charge analysis was conducted, which is given in Table 2 for each of the four reactants.

Table 2: Merz-Kollman (ESP) charges for each of the reactants involved in Schemes 4-6.

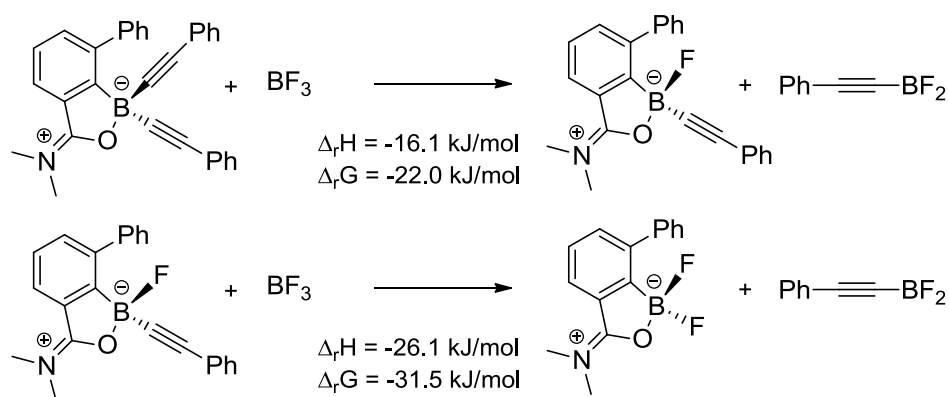
<i>Dienophile</i>	<i>Charge on B</i>	<i>Charge on C₁</i>	<i>Charge on C₂</i>
Alkynylborane (IM)	0.87	-0.37	-0.15
Bis(alkynyl)borane (ID)	0.80	-0.43	0.0
Tris(alkynyl)borane (IT)	0.70	-0.42	0.0
<i>Diene</i>	<i>Charge on O</i>	<i>Charge on C_A</i>	<i>Charge on C_B</i>
2-pyrone (S1)	-0.55	0.43	-0.64

Comparison of all three dienophiles shows that Boron in each case carries a positive charge. However, with additional phenylacetylide groups, this charge is lower. Simultaneously, the negative charge on C₁ increases. Thus, if we only consider electrostatic effects, this would mean that the initial complex will become less stable with an increasing degree of substitution with phenylacetylide groups, which indeed is confirmed by the full energy

profile. At the same, the increasing charge on C₁ (and decreasing charge on C₂) with increasing degree of substitution would lead to more effective nucleophilic attack of C₁ onto C_A, which is apparent in the lowering of the barrier, as is clear from comparing Schemes 4-6. In fact, notwithstanding the fact that one cannot assume these charges to be accurate to 0.01, the slightly lower charge on C₁ for **IT** compared to **ID** suggests a slightly higher barrier, as is clear from Table 1.

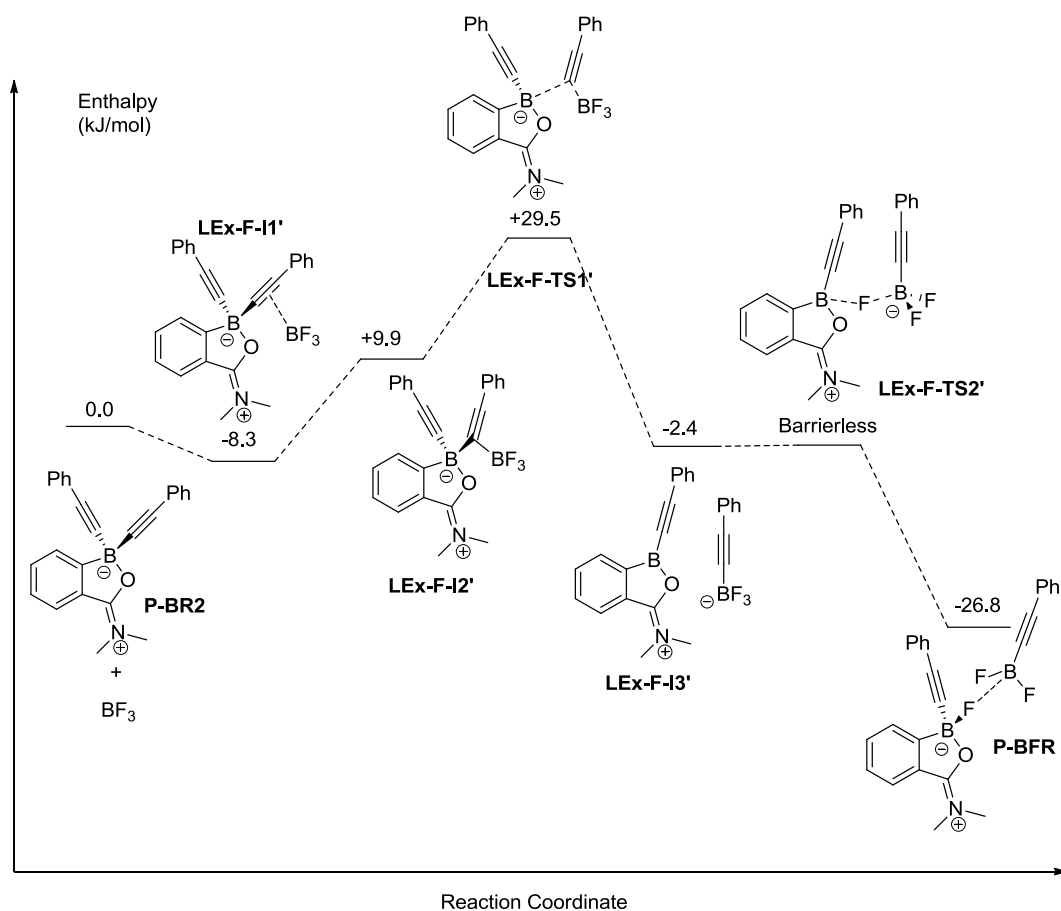
The calculations shown in Table 1 suggest that the cycloadditions should provide a mixture of products favouring mono- and dialkynylated boranes. However, experimental studies show that aryldifluoroboranes are the major products. We speculated therefore that the final stage of the cycloaddition process required a further equilibration of arylboranes, and therefore undertook a study into potential ligand exchange processes in the products. Interestingly, as shown in Scheme 8, calculations show that the boron trifluoride promoted conversion of **P-BR2** via **P-BFR** to **P-BF2** is exothermic. For the first transformation from **P-BR2** to **P-BFR** $\Delta_r H$ and $\Delta_r G$ are -16.1 kJ mol⁻¹ and -22.0 kJ mol⁻¹, respectively. For the final transformation into **P-BF2**, $\Delta_r H$ and $\Delta_r G$ are -26.1 kJ mol⁻¹ and -31.5 kJ mol⁻¹, respectively.

Scheme 7 The ligand (phenylacetylide group) exchange reaction between **P-BR2**, **P-BFR** and BF₃

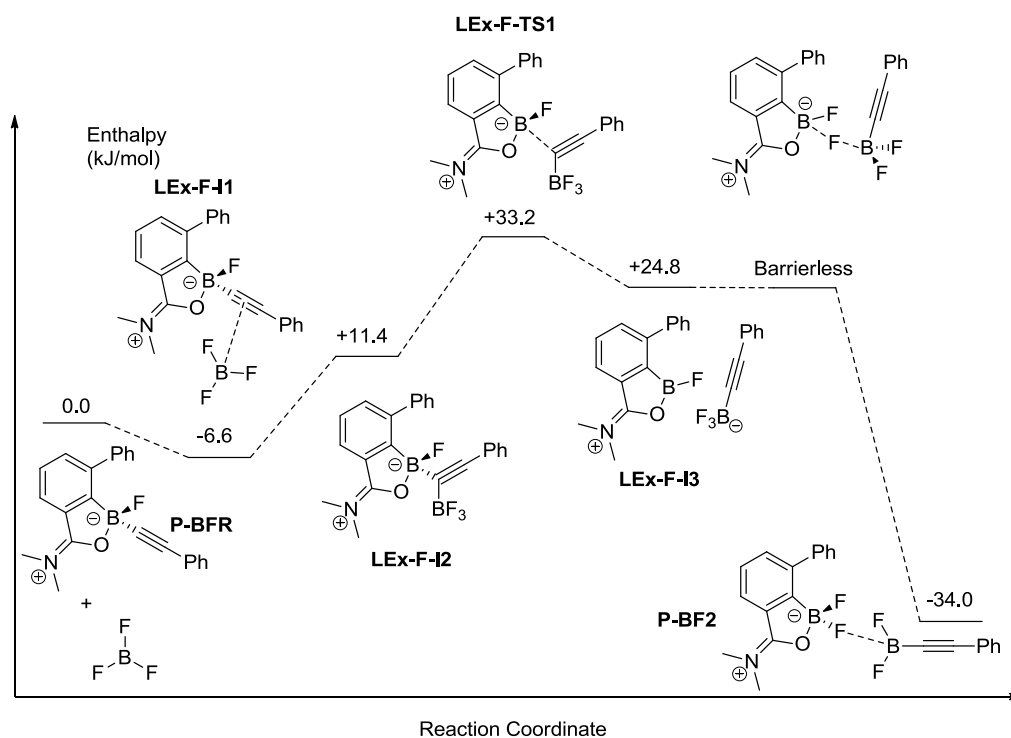


While there does not appear to be a very significant driving force for the equilibration of all possible cycloadducts to the aryldifluoroborane, the presence of excess Lewis acid (remaining after consumption of alkyne during cycloaddition) probably serves to drive this transformation forward. To investigate this further, the energy profile of the equilibration of mono- and di-alkynylated cycloadducts was studied and is depicted in Schemes 8 and 9, respectively.

Scheme 8 The energy profile of the ligand exchange reaction between **P-BR2** and BF_3 . Please note that dissociation of the final complex is endothermic by 10.7 kJ mol^{-1} .

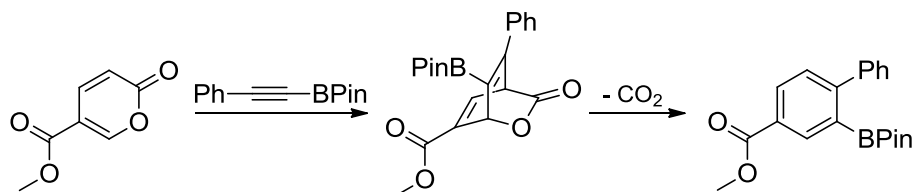


Scheme 9 The energy profile of the ligand exchange reaction between **P-BFR** and BF_3 . Please note that the dissociation of the final complex is endothermic by 7.9 kJ mol^{-1} .



Our calculations clearly show that the formation of **P-BF2** should indeed be quite facile, given the low barriers, which are significantly lower than the corresponding barriers to formation of **ID** and **IT**. Thus, our calculations clearly explain and confirm the experimental observations. However, the above discussion does not consider the role of the directing group and the effect it has on the formation of the final products. Unfortunately, the directing group for 2-pyrone is in such a position, that the study of a non-directed reaction leading to the same products is not feasible. However, one of us has previously reported a non-directed Diels-Alder reaction as a route to synthesize functionalized aromatic boronic esters, as shown in Scheme 10.³¹

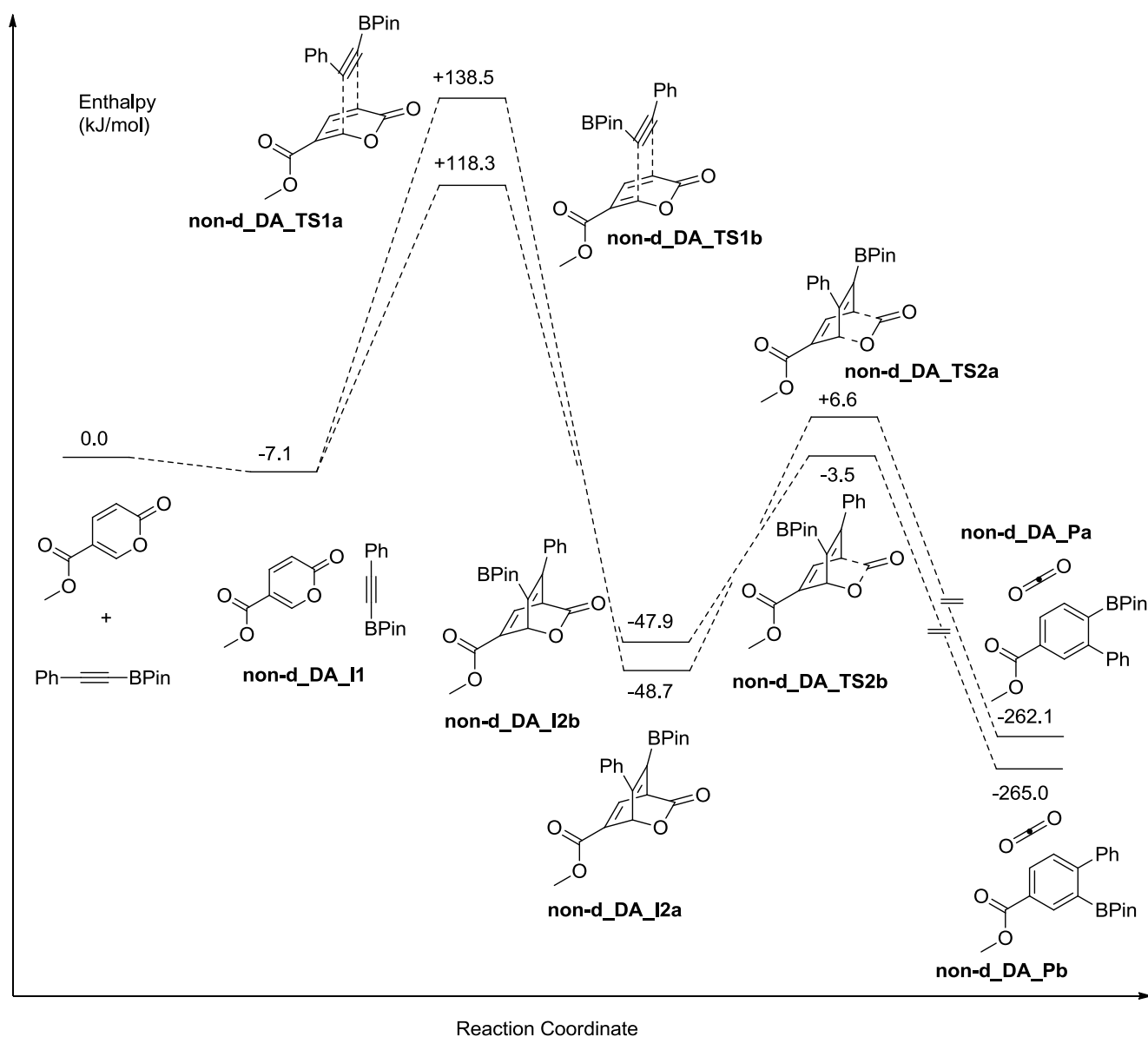
Scheme 10 Alkynylboronate Diels-Alder reaction, where BPin is pinacolborane.



In the case of this non-directed cycloaddition, the reaction conditions are quite harsh and require heating at 180 °C for 18 hours to drive the reaction to completion. Thus, to

understand the role of the directing group and to be able to explain the difference between the non-directed Diels-Alder reaction and the novel mild directed Diels-Alder reaction, we decided to re-examine the MEP for this previously reported non-directed Diels-Alder reaction instead. The enthalpy profile for this reaction was calculated and is shown in Scheme 11.

Scheme 11 The energy profile for the non-directed Diels-Alder reaction as shown in Scheme 10.



Scheme 11 has a similar structure to Schemes 4-6. The initial step in the reaction is the complexation of the two reactants followed by the cycloaddition. In this case the cycloaddition is more synchronous with both C-C bonds forming at approximately the same

time, leading to a bridged intermediate, which will evolve CO₂ to yield the final product. Comparison of Scheme 11 to Schemes 4-6 shows that the effective barrier for the non-directed Diels-Alder reaction pathway is much higher than for the directed Diels-Alder reaction. For the non-directed DA reaction, the TDI is **non-d_DA_I1** for the formation of both products, whereas the TDTS is the cycloaddition transition state in both cases. Thus, the effective barrier to generate the more stable product **Pb** is +118.3 kJ mol⁻¹ whereas it is +138.5 kJ mol⁻¹ for generating the product **Pa**. From Scheme 12, the product **Pb** is predicted to be the dominant product due to the significantly lower barrier, which is also confirmed by the experimental observations.

By considering the effective barriers in the three directed Diels-Alder reactions which were discussed above (varying from 94.0 kJ mol⁻¹ to 99.7 kJ mol⁻¹), it is clear that the non-directed reaction will require harsher conditions. Moreover, it seems therefore unlikely that this mechanism could be in operation in parallel to the directed Diels-Alder reaction.

In order to ensure that the above analysis was not specific to the amide substrate **S1**, all calculations were repeated with the pyridine-pyrone **1**. The complete reaction profiles for these reactions are given in the supporting information. However, the most important data is summarized in Table 3.

Table 3: Comparison of the most relevant enthalpies for the reaction of the three boron-alkynyl species with the amide (**S1**) and pyridine (**1**) substrates. All enthalpies quoted are in kJ mol⁻¹

	amide (S1)	pyridine (1)
$\Delta_r H(\mathbf{P-BF2})$	-334.7	-335.0
$\Delta_r H(\mathbf{P-BFR})$	-318.2	-323.8
$\Delta_r H(\mathbf{P-BR2})$	-298.6	-310.5
$\Delta H^\ddagger(\mathbf{P-BF2})$	99.7	101.4
$\Delta H^\ddagger(\mathbf{P-BFR})$	94.0	91.2
$\Delta H^\ddagger(\mathbf{P-BR2})$	95.7	92.2
$\Delta_r H(\mathbf{P-BR2} \rightarrow \mathbf{P-BFR})$	-16.1	-18.5
$\Delta_r H(\mathbf{P-BFR} \rightarrow \mathbf{P-BF2})$	-26.1	-30.3
$\Delta H^\ddagger(\mathbf{P-BR2} \rightarrow \mathbf{P-BFR})$	29.5	55.4

$\Delta H^\ddagger(\mathbf{P-BFR} \rightarrow \mathbf{P-BF2})$	33.2	62.9
--	------	------

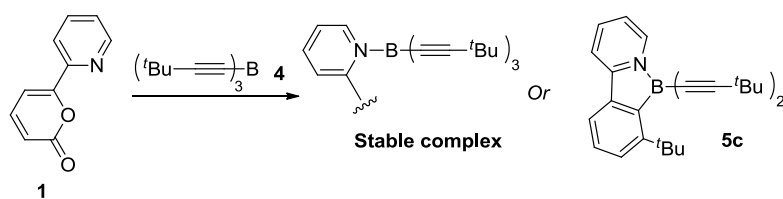
It is clear from the comparison of the enthalpies for the reaction of the boron-alkynyl species with either the 2-pyrone amide (**S1**) or the 2-pyrone pyridine (**1**), that the enthalpic parameters for both reactions are very similar, providing reassurance that the analysis of the reaction with **S1** is applicable to other substrates as well. The calculations also suggest that the reaction with **1** should be faster than the reaction with **S1** under the same conditions. However, the higher barriers for the subsequent disproportionation process back from **P-BR2** to **P-BF2** should lead to higher conversion to difluoroborane in the case of **S1** versus **1**.³²

Overall therefore, our calculations have highlighted three key processes in the boron trifluoride promoted cycloaddition of alkynyltrifluoroborates and 2-pyrones: (1) rapid pre-equilibration of alkynylboranes through ligand exchange. (2) Lewis acid/base complexation of the dienophile/diene, respectively, followed by cycloaddition *via* a [4 + 2] mechanism. (3) Equilibration of cycloadducts to a single product, thereby avoiding the formation of product mixtures. It is clear that the precise Lewis acid used has a significant effect on the effective barriers. Thus, it should be possible to use alternative Lewis acids to modulate these effects, and our investigations towards this end are described later in the next section.

Experimental Results

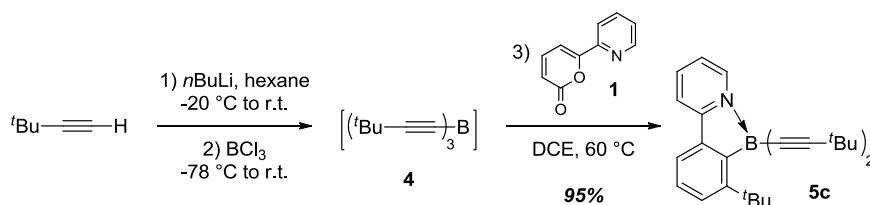
Our computational investigations highlighted the potential of a mechanism that involved rapid and reversible formation of tris(alkynyl)borane, followed by cycloaddition and disproportionation. We wanted to confirm the viability of this mechanism experimentally. In this context, Siebert and co-workers reported the synthesis and characterization of tris(*t*-butynyl)borane **4** as a Lewis acid-base complex with pyridine,³³ and it occurred to us that we could employ this chemistry to probe the key cycloaddition step. More specifically, if the tris(alkynyl)borane was unreactive with pyrone **1**, then we should be able to observe the resulting complex and compare data with that reported by Siebert. However, if the alkyne was reactive, then we would expect to recover the corresponding cycloadduct **5c**. In the event that **5c** was isolated, we could confirm the possibility of the final disproportionation process by subjecting this compound to a boron Lewis acid.

Scheme 12 Synthesis and cycloaddition of a trialkynylborane



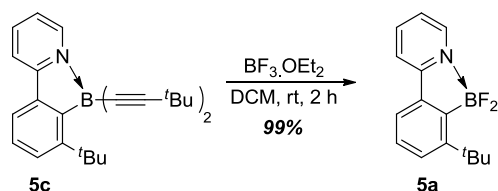
We prepared tris(*t*-butynyl)borane **4** according to the literature procedure and found that it underwent cycloaddition with **1** to generate bis(alkynyl)borane derivative **5c** in 95% yield. Notably, we did not observe any chloroborane derived cycloadducts (Scheme 13). This result supported our computational calculations in which the tris(alkynyl)borane derivative functions as a 2π component in the $[4 + 2]$ cycloaddition between 2-pyrones and potassium (alkynyl)trifluoroborate salts.

Scheme 13 Synthesis and cycloaddition of a trialkynylborane



Further control experiments were carried out to validate the possibility of the final disproportionation step (Scheme 14). We first verified that difluoroborane complex **5a** was obtained upon exposure of bis(alkynyl)borane derivative **5c** to boron trifluoride (Scheme 14). The observation that this process takes place smoothly at room temperature matches the results of our theoretical study that predict the barrier of ligand exchange between BF_3 and products to be quite small (c.f. Scheme 7).

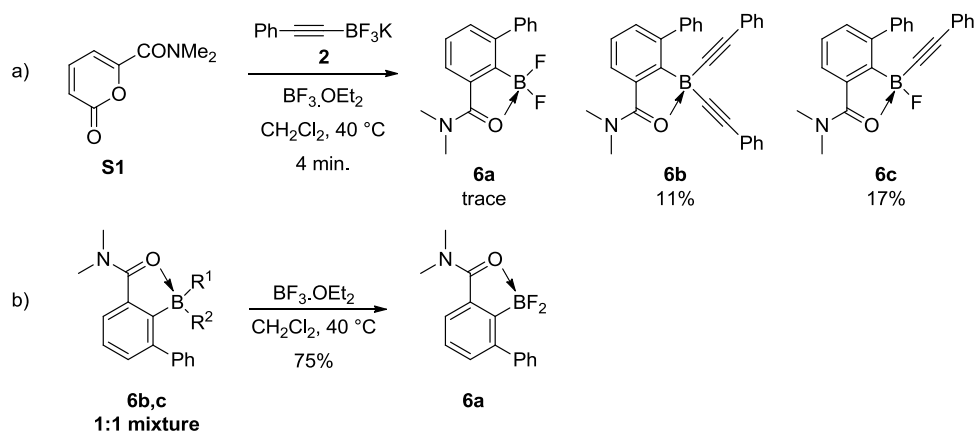
Scheme 14 Equilibration of dialkynylborane to difluoroborane



In order to demonstrate the generality of the disproportionation process, complexes **6b** and **6c** were also prepared (Scheme 15). Treating pyrone **S1** with trifluoroborate salt **2** in the presence of boron trifluoride for 4 minutes led to the isolation of **6b** and **6c** in 11% and 17% yield, respectively (Scheme 16a).³⁴ As expected, difluoroborane **6a** was isolated in 75% yield

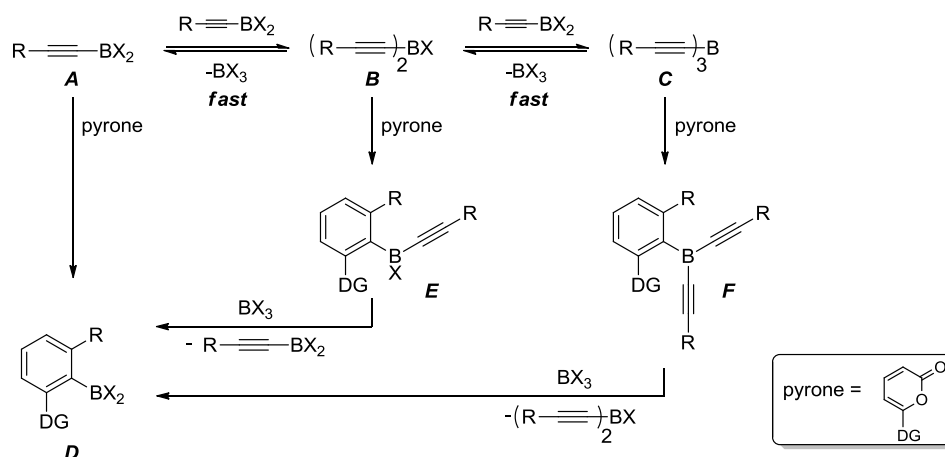
when a 1:1 mixture of **6b** and **6c** was treated with boron trifluoride, further validating the computational results (Scheme 15b).

Scheme 15 Equilibration of alkynylboranes to difluoroborane.



Both theoretical and experimental results allow us to propose a mechanism accounting for the transformation (Scheme 16). A rapid equilibrium between (alkynyl)dihalogenoborane **A**, bis(alkynyl)halogenoborane **B** and tris(alkynyl)borane **C** followed by the [4 + 2] cycloaddition between the 2-pyrone and each borane derivative affords cycloadducts **D**, **E** and **F**, respectively. Finally, intermediates **E** and **F** are converted into dihalogenoborane cycloadduct **D** by reacting with BX_3 .

Scheme 16 Overall mechanistic scheme for the directed cycloaddition reaction.

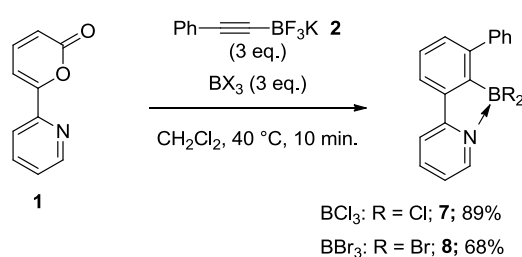


Extension of the methodology using BCl_3

Our theoretical studies indicated that the precise Lewis acid used has a significant effect on the effective barrier for this reaction. Thus, as implied in the mechanism shown in Scheme

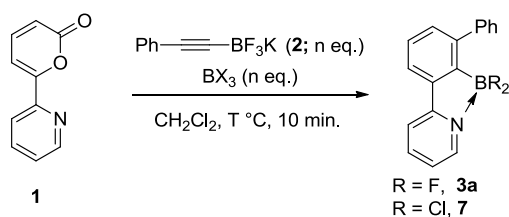
16, it seemed logical that other boron trihalides (BX_3) could act as suitable Lewis acids to promote the cycloaddition process. Indeed, we found that both BCl_3 and BBr_3 can function as effective promoters of the cycloaddition (Scheme 17). Using the reaction conditions initially reported in our previous study (i.e. 3 equivalents of potassium (alkynyl)trifluoroborate **2**, 3 equivalents of Lewis acid in refluxing CH_2Cl_2),⁹ cycloadducts **7** and **8** were isolated in 89% and 68% yield, respectively.

Scheme 17 Use of alternative BX_3 promoters



As BCl_3 appeared to be more promising, an optimization study was carried out on the cycloaddition of **1** and **2** (Table 4). Interestingly, we found that the temperature of reaction could be reduced to rt or 0 °C without affecting the yield of isolated product (entries 3 and 4). Furthermore, the number of equivalents of alkyne and BCl_3 could be reduced without significantly reducing the yield of **7** when the reaction was carried at 0 °C (entry 6). This temperature was found to be optimal since higher or lower reaction temperature (entries 5 and 7) led to the decrease of isolated yield of **7**. Further reduction of the number of equivalents of alkyne and BCl_3 gave incomplete conversions after prolonged reaction times. Overall, this study demonstrated that higher reactivity could be achieved when BCl_3 was used as the reaction promoter.

Table 4 Lewis acid screening.

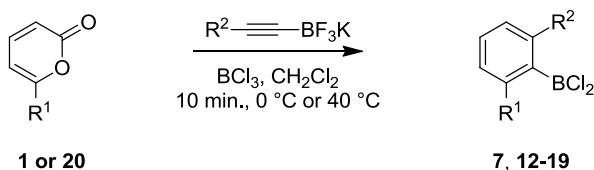


Entry	BX ₃	alkyne / BX ₃ n eq. / n eq.	T °C	R	Isolated yield %
1	BF ₃	3 / 3	40	F	82%
2	BCl ₃	3 / 3	40	Cl	89%
3	BCl ₃	3 / 3	r.t.	Cl	84%
4	BCl ₃	3 / 3	0	Cl	93%
5	BCl ₃	2 / 2	r.t.	Cl	68%
6	BCl ₃	2 / 2	0	Cl	84%
7	BCl ₃	2 / 2	-15	Cl	78%

initial conditions

The reaction scope was next investigated using our optimized conditions (i.e. 2 equivalents of potassium alkynyltrifluoroborate and 2 equivalents of BCl₃). First, we prepared a series of potassium alkynyltrifluoroborate salts and used them in the cycloaddition reaction with 2-pyrones **1** and (Table 4). In both cases, similar trends were obtained. Alkyne substrates bearing phenyl-, ⁿbutyl- and ^tbutyl-substituents reacted rapidly under mild conditions to give the corresponding functionalised aromatic products **7**, **12-19** in good to excellent yields (entries 1-8). The combination of thiazole-substituted 2-pyrone **20** and TMS-alkyne **11** resulted in a slower reaction and this process was conducted at slightly elevated temperature, resulting in some protodesilylation of the product.

Table 5 Cycloaddition scope



Entry	Pyrone	R ²	T °C	Product	Isolated yield	Entry	Pyrone	R ²	T °C	Product	Isolated yield
1		Ph- (2)	0 °C	7	84%	6		Ph- (2)	0 °C	16	83%
2		ⁿ Bu- (8)	0 °C	12	89%	7		ⁿ Bu- (8)	0 °C	17	97%
3		^t Bu- (9)	0 °C	13	70%	8		1-cyclohexenyl- (10)	0 °C	18	84%
4	1	1-cyclohexenyl- (10)	0 °C	14	54%	9	20	TMS- (11)	40 °C	19	51% ^a
5	1	TMS- (11)	0 °C	15	47%						

^aThe product of protodesilylation was also observed in 18% yield.

The cycloaddition of 2-pyrones attached at the 4-position of various 1,3-azoles groups was found to be more challenging, and these reactions were generally conducted at elevated temperature (Table 6). Nonetheless, these reactions allow a range of biaryl products to be accessed in good yield. Pyrone **21**, which is a regioisomer of pyrone **20** in Table 5, also underwent the cycloaddition with alkynes **2**, **8** and **10** (entries 1-3). Pyrone **22**, having a 2-methyloxazole as directing group, was also efficient under our reaction conditions, affording products **27-29** in good yields (entries 4-6). Interestingly, a small change in the 2-methyloxazole motif showed a dramatic change in reactivity; 2-pyrone **23** proved to be reluctant to undergo the cycloaddition, requiring a reaction time of 3 days and affording cycloadducts **30-32** in modest yields (entries 7-9). Notably however, attempts to mediate the reaction of **23** and **2** with $\text{BF}_3 \cdot \text{OEt}_2$ failed to deliver any product and only starting 2-pyrone was returned in this case, highlighting the potential of BCl_3 to offer enhanced reactivities.

Table 6 Cycloaddition scope

Entry	Pyrone	R ²	time	Product	Isolated yield
1		Ph- (2)	10 min.	24	77%
2		ⁿ Bu- (8)	10 min.	25	75%
3		1-cyclohexenyl- (10)	10 min.	26	67%

4		Ph- (2)	10 min.	27	76%
5		ⁿ Bu- (8)	10 min.	28	78%
6		1-cyclohexenyl- (10)	10 min.	29	48%

7		Ph- (2)	3 d.	30	55%
8		ⁿ Bu- (8)	3 d.	31	53% ^a
9		1-cyclohexenyl- (10)	3 d.	32	42% ^a

^aThese reactions failed to reach full conversion.

Conclusion

We have carried out theoretical and experimental studies of the mechanism of a Lewis acid promoted cycloaddition of alkynyltrifluoroborates and 2-pyrones bearing a Lewis base promoter. Calculations show that rapid equilibration of in situ generated alkynyl difluoroboranes takes place to provide low concentrations of the corresponding di- and

trialkynylboranes. These latter two species undergo very rapid reaction via coordination of the Lewis basic donor and a [4 + 2] cycloaddition, followed by disproportionation to generate the observed aryl difluoroboranes products. The reactions can be further enhanced by the use BCl₃, allowing cycloaddition to take place within 10 minutes at 0 °C to generate a range of functionalized aromatic products in high yield.

Supporting information

The supporting information contains general experimental protocols and NMR spectra. Computational supporting data includes Cartesian coordinates (in XYZ format) and energies. This material is available free of charge via the Internet at <http://pubs.acs.org>.

Acknowledgements

We are grateful to AstraZeneca, EPSRC, and The University of Sheffield for financial support. All calculations were performed on the “Jupiter” cluster of the Theoretical Chemistry Group at the University of Sheffield as well as the central “Iceberg” cluster of the University of Sheffield. The authors thank Mr. Christopher M. Parks for useful discussions and help with the calculations.

References

1. Woodard, B. T.; Posner, G. H. *Adv. Cycloadd.* **1999**, 5, 47.
2. Diels O.; Alder, K. *Ann. Chem.* **1931**, 490, 257.
3. Afarinkia, K.; Vinader, V.; Nelson, T. D.; Posner, G. H. *Tetrahedron* **1992**, 48, 9111.
4. (a) Delaney, P. M.; Moore, J. E. *Chem. Commun.* **2006**, 42, 3323; (b) Delaney, P. M.; Browne, D. L.; Adams, H.; Plant, A.; Harrity, J. P. A. *Tetrahedron* **2008**, 64, 866.
5. Evnin, A.; Seyferth, D. J. *Org. Chem.* **1967**, 32, 952.
6. Seyferth, D.; White D. J. *Organomet. Chem.* **1972**, 34, 119.
7. Kranjc, K.; Štefane, B.; Polanc, S.; Kočevar, M. J. *Org. Chem.* **2004**, 69, 3190.
8. Vivat, J. F.; Adams, H.; Harrity, J. P. A. *Org. Lett.* **2010**, 12, 160.
9. Kirkham, J. D.; Butlin, R. J.; Harrity, J. P. A. *Angew. Chem. Int. Ed.* **2012**, 51, 6402.
10. (a) Singleton, D. A.; Martinez, J. P. J. *Am. Chem. Soc.* **1990**, 112, 7423; (b) Singleton, D. A. J. *Am. Chem. Soc.* **1992**, 114, 6563; (c) Leung, S.-W.; Singleton, D. A. J. *Org. Chem.* **1992**, 57, 4796; (d) Leung, S.-W.; Singleton, D. A. J. *Org. Chem.* **1997**, 62, 1955.
11. See e.g. (a) Sakata K.; Fujimoto H. *J. Org. Chem.* **2013**, 78, 3095; (b) Pham, H. V.; Paton, R. S.; Ross, A. G.; Danishefsky, S. J.; Houk, K. N. *J. Am. Chem. Soc.* **2014**, 136, 2397; (c) Birney, D. M.; Houk, K. N. *J. Am. Chem. Soc.*, **1990**, 112, 4127; (d) Domingo, L. R.; Arnó, M.; Sáez, J. A. *J. Org. Chem.* **2009**, 74, 5934; (e) Domingo, L. R. *Organic Chemistry: Current Research* **2013**, 2, 120; (f)

- Soto-Delgado, J.; Saez, J. A.; Tapia, R. A.; Domingo, L.R. *Org. Biomol. Chem.* **2013**, *11*, 8357; (g) Arno, M.; Picher, M. T.; Domingo, L. R.; Andres, J. *Chem. Eur. J.* **2004**, *10*, 4742; (h) Sarotti, A. M. *Org. Biomol. Chem.* **2014**, *12*, 187; and references therein.
12. (a) Becke, A. D. *Phys. Rev. A*, **1988**, *38*, 3098; (b) Becke, A. D. *J. Chem. Phys.*, **1993**, *98*, 1372.
13. Lee, C.; Yang, W.; Parr, R. G. *Phys. Rev. B*, **1988**, *37*, 785.
14. Gaussian 09, Revision D.01, Frisch, M. J.; Trucks, G. W.; Schlegel, H. B.; Scuseria, G. E.; Robb, M. A.; Cheeseman, J. R.; Scalmani, G.; Barone, V.; Mennucci, B.; Petersson, G. A.; Nakatsuji, H.; Caricato, M.; Li, X.; Hratchian, H. P.; Izmaylov, A. F.; Bloino, J.; Zheng, G.; Sonnenberg, J. L.; Hada, M.; Ehara, M.; Toyota, K.; Fukuda, R.; Hasegawa, J.; Ishida, M.; Nakajima, T.; Honda, Y.; Kitao, O.; Nakai, H.; Vreven, T.; Montgomery, J. A., Jr.; Peralta, J. E.; Ogliaro, F.; Bearpark, M.; Heyd, J. J.; Brothers, E.; Kudin, K. N.; Staroverov, V. N.; Kobayashi, R.; Normand, J.; Raghavachari, K.; Rendell, A.; Burant, J. C.; Iyengar, S. S.; Tomasi, J.; Cossi, M.; Rega, N.; Millam, J. M.; Klene, M.; Knox, J. E.; Cross, J. B.; Bakken, V.; Adamo, C.; Jaramillo, J.; Gomperts, R.; Stratmann, R. E.; Yazyev, O.; Austin, A. J.; Cammi, R.; Pomelli, C.; Ochterski, J. W.; Martin, R. L.; Morokuma, K.; Zakrzewski, V. G.; Voth, G. A.; Salvador, P.; Dannenberg, J. J.; Dapprich, S.; Daniels, A. D.; Farkas, Ö.; Foresman, J. B.; Ortiz, J. V.; Cioslowski, J.; Fox, D.J. Gaussian, Inc., Wallingford CT, **2009**.
15. Peng, C.; Schlegel, H. B. *Israel J. Chem.*, **1993**, *33*, 449.
16. Peng, C.; Ayala, P. Y.; Schlegel, H. B.; Frisch, M. J. *J. Comp. Chem.*, **1996**, *17*, 49.
17. Cancès, M. T.; Mennucci, B.; Tomasi, J. *J. Chem. Phys.*, **1997**, *107*, 3032.
18. Schlegel, H. B. *J. Comp. Chem.*, **1982**, *3*, 214.
19. Fukui, K. *Acc. Chem. Res.*, 1981, *14*, 363.
20. Mennucci, B.; Tomasi, J. *J. Chem. Phys.*, **1997**, *106*, 5151.
21. Cossi, M.; Barone, V.; Mennucci, B.; Tomasi, J. *Chem. Phys. Lett.*, **1998**, *286*, 253.
22. Cossi, M.; Scalmani, G.; Rega, N.; Barone, V. *J. Chem. Phys.*, **2002**, *117*, 43.
23. Sing, U. C.; Kollman, P. A. *J. Comput. Chem.*, **1984**, *5*, 129.
24. Besler, B. H.; Merz, K. M.; Kollman, P. A. *J. Comput. Chem.*, **1990**, *11*, 217.
25. Bardin, V. V.; Adonin, N. Y.; Frohn, H.-J. *J. Fluor. Chem.* **2007**, *128*, 699.
26. Negishi, E.-i.; Idacavage, M. J.; Chiu, K.-W.; Yoshida, T.; Abramovitch, A.; Goettel, M. E.; Silveira, A.; Bretherick, H. D. *J. Chem. Soc., Perkin Trans. 2* **1978**, 1225.
27. (a) Cao, Y.; Osuna, S.; Liang, Y.; Haddon, R. C.; Houk, K. N.; Braunschweig, A. B. *J. Am. Chem. Soc.* **2013**, *135*, 9240; (b) Štefane, B.; Perdih, A.; Pevec, A.; Šolmajer, T.; Kočever, M. *Eur. J. Org. Chem.* **2010**, 5870; (c) Kranjc, K.; Kočever, M. *New J. Chem.* **2005**, *29*, 1027.
28. Kozuch, S.; Shaik, S. *Acc. Chem. Res.* **2011**, *44*, 101.
29. Kozuch, S.; Martin, J. M. L. *ChemPhysChem.* **2011**, *12*, 1413.
30. Kozuch, S. *WIREs Comput. Mol. Sci.* **2012**, *2*, 795.
31. Kirkham, J. D.; Leach, A. G.; Row, E. C.; Harrity, J. P. A. *Synthesis* **2012**, *44*, 1964.
32. This is indeed what is found experimentally. If **S1** is mixed with **IM1** for 40 minutes at room

temperature, 70% conversion is obtained with 80% **P-BF2** and 20% **P-BFR** and only traces of **P-BR2**. If instead **1** is mixed with **IM1** under the same conditions, then 92% conversion is achieved with 45% **P-BF2**, 27% **P-BFR**, and 28% **P-BR2** (as estimated by 400 MHz ¹H NMR spectroscopy of crude reaction mixtures).

33. Bayer, M. J.; Pritzkow, H.; Siebert, W. *Eur. J. Org. Chem.* **2002**, 2069.

34. The low yields observed in this case can be attributed to the fact that several purifications by column chromatography were required to obtain **8b** and **8c** as clean products.